

Ultrafast dynamics of silver nanoparticle shape transformation studied by femtosecond pulse-pair irradiation

A. Akin Unal, A. Stalmashonak, G. Seifert, and H. Graener*

Institut für Physik, Fachgruppe Optik, Martin-Luther-Universität, Hoher Weg 8, 06120 Halle, Germany

(Received 3 December 2008; published 12 March 2009)

Spherical silver nanoparticles embedded in glass were irradiated by pairs of time-delayed laser pulses with equal intensities resulting in delay-dependent nanoparticle shape transformations. The corresponding persistent changes in the surface-plasmon extinction bands are analyzed as a function of time delay and relative polarization of the pulse pairs. We find that the strongest nanoparticle shape changes, i.e., the highest aspect ratios, are achieved when the delay between pulse pairs is less than 3 ps. After 10 ps the dichroism is strongly reduced in the case of pulse pairs having identical polarization and vanishes using pulse pairs with orthogonal polarization. Using an extended two-temperature model, the time dependence of directed and isotropic thermal electron emissions was estimated to decay on a time scale of a few picoseconds. Our results strongly suggest that the electron and following ion emission from the nanoparticles are finished within less than 20 ps, and the directional memory is favorably defined by directed emission of hot electrons interacting with the laser field.

DOI: [10.1103/PhysRevB.79.115411](https://doi.org/10.1103/PhysRevB.79.115411)

PACS number(s): 78.67.Bf, 73.20.Mf, 79.20.Ds, 65.80.+n

I. INTRODUCTION

Dielectric materials containing metallic nanoparticles (NPs) are still a subject of widespread interest owing to their unique linear and nonlinear optical properties.¹⁻⁴ The resonant interaction of light with metallic NPs is described by the collective oscillation of conduction electrons, which are localized at the interface of the NP and the surrounding dielectric. These charge-density oscillations, usually called surface-plasmon (SP) resonances, are responsible for high local fields and specific extinction bands. The spectral features of the latter depend strongly on the size and shape of the NP, as well as on the dielectric properties of the surrounding environment.

High intensity femtosecond (fs) laser irradiation of composite glass containing silver NPs was shown to cause optical dichroism by permanent NP shape modifications.^{5,6} Linearly polarized laser irradiation can transform initially spherical silver NPs into elongated shapes with their symmetry axes oriented along the polarization direction of the laser. Due to this shape modification the original SP resonance splits into two spectrally separated bands, caused by electron oscillations parallel or perpendicular to the symmetry axis of the modified NP. The spectral separation between SP resonances depends strongly on the aspect ratio, which is defined as the length of the modified NP divided by its width.

Most of the time-resolved investigations until now were focused on the weak excitation regime (showing only transient SP changes).⁷⁻⁹ However, the physical situation of strong excitation—leading to persistent changes—is of high interest both for fundamental reasons and for potential device applications (allowing, e.g., tailoring of linear and nonlinear optical properties of materials). While the permanent changes have already been studied extensively with respect to the irradiation parameters,^{10,11} there are only few investigations in the strong excitation regime toward understanding in detail the ultrafast dynamics of laser-induced NP shape modification.¹²⁻¹⁴ The underlying central question is how a femtosecond laser pulse can create a directional memory

lasting long enough to steer material transport in a way that NP anisotropy oriented along the polarization direction of the laser pulses is prepared.

In this work we present a different approach in investigating these ultrafast mechanisms by performing fs pulse-pair irradiation experiments. Discussing these results, it will be shown that the emission and trapping of electrons in the matrix are the first and decisive processes initiating the NP anisotropy. The next step in the cascade of processes leading to NP reshaping—ion emission—obviously also occurs in the first few picoseconds.

II. LASER PULSE INTERACTION WITH NANOPARTICLES

The very strong oscillating electric field of an intense fs laser pulse is further enhanced in the near-field region around the NP by typically two orders of magnitude.^{3,15} In the case of resonant interaction with the NP, this effect also enhances the SP oscillation amplitudes with the consequence that the initially collective charge-density oscillations are perturbed by direct electron emissions from the NP. This is the fastest damping mechanism of the SP oscillations occurring from the first plasmon oscillation period onward.^{1,16} The electrons that do not undergo the emission relax into a quasiequilibrated hot electronic system via electron-electron and electron-surface scatterings.^{16,17} For small NPs (diameter less than a few tens of nanometers), this happens within less than one hundred fs.¹⁷

After establishing a thermal electronic system, the hot electrons cool down by sharing their energy with the lattice via electron-phonon (*e-ph*) coupling, thereby heating up the NP. The heat gained by the lattice can be calculated from the heat lost by the electrons using the two-temperature model (TTM),¹⁸ where the heat flow between two subsystems (electron and lattice) is defined by two coupled heat equations. The electron system is characterized by an electron temperature T_e and the phonon system by a lattice temperature T_l , where the *e-ph* coupling factor $G(T_e)$ is responsible for the

energy transfer between two subsystems. The heat equations describing the temporal evolution of T_e and T_l are

$$C_e(T_e) \frac{\partial T_e}{\partial t} = -G(T_e)(T_e - T_l) + S(t), \quad (1)$$

$$C_l \frac{\partial T_l}{\partial t} = G(T_e)(T_e - T_l) - C_l(T_l - T_0)/\tau_s, \quad (2)$$

where $C_e(T_e)$ and C_l are the electronic and lattice heat capacities, respectively. $S(t)$ in the first equation is a source term of Gaussian shape describing the absorbed laser-pulse energy per NP, which is given as

$$S(t) = I(\sigma_{\text{abs}}/V_{\text{NP}}) \exp[-4 \ln(2t/\tau_{\text{FWHM}})^2]. \quad (3)$$

Here I is the peak pulse intensity, σ_{abs} is the absorption cross section of a single silver NP ($\approx 3000 \text{ nm}^2$ in a dielectric environment with a refractive index of $n=1.52$),¹⁹ V_{NP} the volume of the NP, and τ_{FWHM} determines the full width at half maximum of the temporal pulse profile. The last term of Eq. (2) represents heat transfer from the NP to the surrounding glass matrix (with a cooling time constant τ_s) having initially $T=T_0$.

The absorption of an intense fs laser pulse (having energy $\hbar\omega_L$) creates a strongly athermal electron distribution, which is sketched by the arrows in the inset of Fig. 1(a). Electrons having energies between $E_F - \hbar\omega_L$ and E_F are excited above the Fermi level to final energies between E_F and $E_F + \hbar\omega_L$. By the following fast thermalization of these high energetic electrons, a Fermi distribution with a very high electronic temperature is achieved. This shows that the strong laser irradiation of the NP creates huge electron-phonon nonequilibrium conditions, where the high-energy fs pulse raises T_e by several thousands of Kelvins while the lattice still remains cold. As a result of such high temperatures, the thermophysical properties of the NP can be affected by the influence of core d -band electrons, which are located $\sim 3 \text{ eV}$ below the Fermi level in silver.²⁰ The excitation of these electrons is expected to cause significant changes in the electron heat capacity and electron-phonon coupling factor. Therefore, the commonly used literature values of a linear temperature dependence of the C_e and a temperature independent constant value of G are inappropriate for the description of the strong irradiation regime. To account for this fact and to avoid an overestimation of electron temperatures, we have considered the nonlinear temperature dependences of C_e and G factors for silver as they are stated in Ref. 20. In contrast, for the heat capacity of the silver lattice (C_l), the room-temperature value ($3.5 \times 10^6 \text{ J m}^{-3} \text{ K}^{-1}$) is a reasonable approximation because it is known that the change in C_l upon temperature increase by 1500 K is less than 20%.²¹

As an illustration to this ‘‘strong irradiation’’ regime, Fig. 1(a) depicts the results of TTM calculations for the case of a single silver NP excited by a 100 fs pulse with intensity of 0.3 TW/cm^2 (needed for permanent NP shape modification¹¹) and central wavelength of 400 nm ($\hbar\omega_L = 3.1 \text{ eV}$), i.e., close to the SP resonance. It is easily seen that, upon absorbing the laser-pulse energy, the conduction electrons of the NP gain very high temperatures (up to

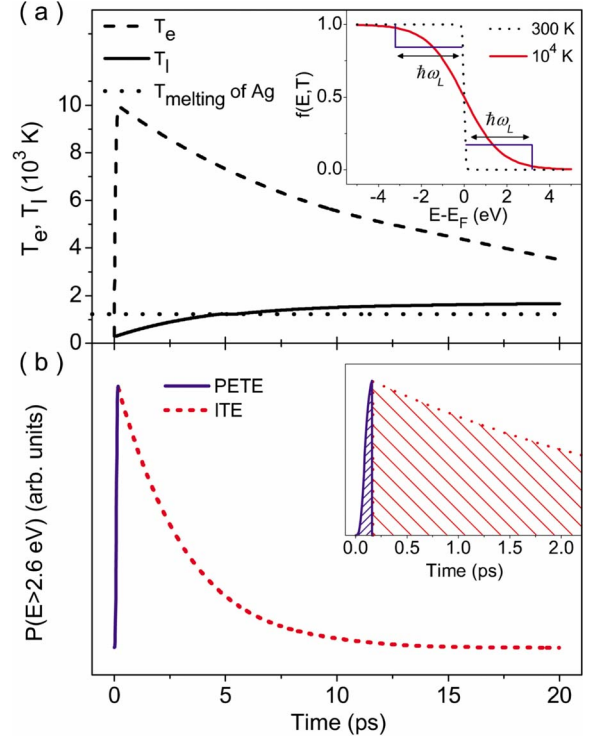


FIG. 1. (Color online) (a) Time evolution of electronic and lattice temperatures of a silver NP following the absorption of an intense fs laser pulse. Inset of (a): changes in Fermi distribution upon laser irradiation. (b) Probabilities of electrons that possess energies above 2.6 eV as a function of time. PETE happens during the pulse (rising curve) and ITE after the pulse (decaying curve). Inset of (b): first 2 ps of PETE and ITE with shaded areas showing the total probabilities for both processes.

10^4 K) within the pulse. It should be noted that these calculations do not include possible energy losses due to electron emission processes. Reaching the maximum T_e , the hot electronic system heats the cold silver lattice to a region of temperatures above the melting point of (bulk) silver within a few picoseconds.

What happens to the NPs after that time? From luminescence and extinction spectra,²² we know that Ag ions are being emitted into the glass matrix upon fs laser irradiation. Transmission electron microscopy (TEM) pictures^{6,10,11} showed that this ion emission leads to partial dissolution of the NPs, creating small Ag aggregates around the remaining NP. So it is obvious that after a few picoseconds already some electrons have left the NP, i.e., the nanoparticle is then positively charged and very hot; electric potential and thermal energy can overcome the binding energy of Ag ions, which are being emitted into the surrounding glass matrix.^{12,13,16,22} As a result of this relaxation mechanism, the total volume of the NP is reduced over time. In addition, part of the energy will be taken from the NP and, via kinetic energy of the ions, be transferred to the glass when the ions are trapped there, which is an additional cooling mechanism of the NP.

If these evidently occurring electron and ion emission processes would be purely thermal, the anisotropy of the NPs after irradiation could not be explained. Therefore, we have

to investigate the possible electron emission processes in more detail, in particular those happening during the pulse interaction because the strong field of a linearly polarized laser pulse is the only reasonable source of a directional preference. According to Mie theory,²³ the SP oscillations of spherical particles are either dipolar or multipolar in character depending on their sizes.²⁴ For particles having sizes much smaller than the wavelength of the exciting electromagnetic field ($d \ll \lambda$), it is sufficient to consider only the first term of the multipolar expansion, i.e., the dipolar term. In this case of small enough NPs, hot electrons can be injected into the surrounding glass matrix along the direction of the laser polarization during interaction with the applied pulse. The probability of this process is clearly correlated with the availability of electronic states of the surrounding medium.

In the case of Ag NPs embedded in glass, the occupied states of the NP coincide in their energy with the electronic states of the glass.^{1,25} The valence-band maximum of the glass lies 10.6 eV below vacuum energy (i.e., -10.6 eV) and has no influence on the silver nanoparticle SPs. On the other hand, the lowest conduction band of the glass occurs around -1.7 eV. Comparing this with the Fermi level of Ag, which lies at -4.3 eV, yields a 2.6 eV gap in between the Fermi level of the silver NPs and the conduction band of the glass matrix. This energy is lower than the SP resonance energy of the Ag NPs in glass ($\hbar\omega_{SP} \approx 3$ eV). This shows that it is possible for a SP to decay by injection of a hot electron (with $E \geq 2.6$ eV) into the glass conduction band.²⁵ Therefore, our irradiation at 3.1 eV, which is very close to the SP resonance, can provide considerable probability for the NP electrons to penetrate into the glass conduction band(s) within the pulse duration.

The case depicted in the inset of Fig. 1(a) shows the Fermi distribution of an electronic system upon absorbing the $\hbar\omega_L = 3.1$ eV laser pulse. It is seen that the high-energy tail of the Fermi distribution with $T_e \approx 10^4$ K exceeds the energy needed for NP electrons to penetrate into the glass conduction band (2.6 eV). It is obvious regarding this Fermi distribution that NPs can inject hot electrons into the glass during and after the laser-pulse interaction. This gives rise to two different types of electron emission processes, which we will classify as “pulse enhanced” or “purely thermal” in the following.

Electrons being emitted during the laser-pulse interaction will be driven by the strong oscillating electric field and therefore generate an anisotropic distribution of emission directions, obviously given by the electric field oscillations (polarization) of the laser pulse. The anticipated 100 fs pulses at $\lambda = 400$ nm correspond to 75 full oscillation cycles with mostly very high amplitudes. A simple estimate shows that a conduction-band electron of the NP can gain a linear acceleration of around 10^{20} m/s² upon encountering a linear-polarized pulse of 0.3 TW/cm² intensity (corresponding to an electric field amplitude of 10^9 V/m) within the half plasmon period. In the absence of any damping, this acceleration can push the electron approximately 0.1 nm away from the NP surface. The enhanced electric field at the particle-glass interface^{3,15} can increase this value to approximately 10 nm. Electrons driven so far away from the NP

have left the region of the strongest field enhancement, will thus experience a weaker backward force due to the reversed field of the next half plasmon period, and may finally be trapped in the glass matrix. These numbers make plausible that under the specified conditions there is a non-negligible probability for emission of even “cold” electrons. This direct field-driven electron emission has also been shown by theoretical works for Na clusters.¹⁶

With increase in the absorbed energy, the remaining electrons gain high temperatures and start to build up a Fermi distribution via e - e collisions. The increasing electron temperature produces a significant number of electrons at energies matching the glass conduction band. This will greatly enhance the probability of anisotropic electron emissions from the NP although it remains an open question if at very high electron temperatures the simple picture of a collective plasmon oscillation is still correct. Since, however, the details of these processes are not relevant for this work, we will in the following comprise all field-driven directed electron emissions from NPs occurring during interaction with a laser pulse by the notion “pulse-enhanced thermal emission” (PETE). When the laser pulse is terminated, the electronic system is still very hot, and thus there are still enough electrons at energies allowing them to enter the glass conduction band just by a diffusive process. In contrast to the pulse-enhanced processes (PETE), these purely temperature-driven electron emissions are isotropic. We will call this comparably long-lived process isotropic thermal emission (ITE) of electrons. For all the emitted electrons there is a certain probability that they lose their energy rapidly and are eventually trapped at local potential minima forming color centers in the glass.²² These trapped electrons play an important role in reducing Ag cations at later times.

To get a better understanding of the time evolution of the thermal emission processes, we calculated the Fermi distribution as a function of T_e , and used the resulting amount of electrons above 2.6 eV as an estimate for the relative electron emission probabilities. Figure 1(b) shows this percentage of electrons, referring to the situation of Fig. 1(a) as a function of time. During the time of the laser pulse, we add probability to the PETE process (blue solid line) while after the end of the pulse the percentage of high-energy electrons is assigned to add probability to the ITE process (red dotted line). Thus, integration over the pulse duration (start and end of pulse defined by $1/e^2$ intensity) and the whole remaining time interval afterward yields the total relative probabilities (ΣP) of the two processes. These integrals are shown as shaded areas under the curves in the inset of Fig. 1(b). The absolute probabilities are unknown but it is obvious to anticipate higher probability for the PETE process to account for the experimentally observed anisotropy.

III. EXPERIMENTAL

The samples studied here consist of a 1-mm-thick soda-lime glass containing spherical silver NPs in a thin surface region of 2–3 μ m. The average radius of the NPs is around 15 nm, at a volume filling factor of 10^{-3} . Thus interaction between the NPs can be neglected. The NPs exhibit a sharp SP resonance centered at around 413 nm.

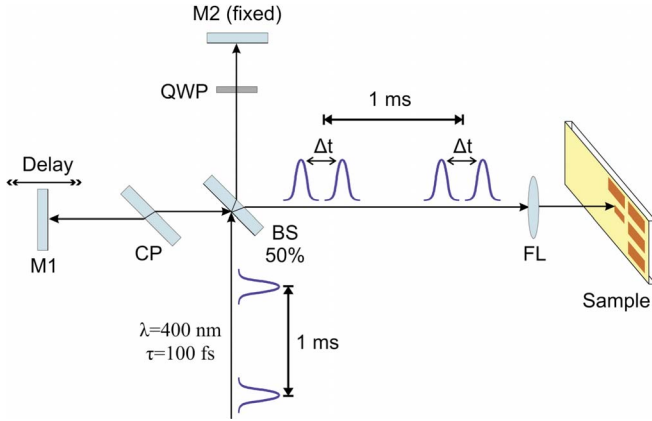


FIG. 2. (Color online) Irradiation by time-delayed pulse pairs. BS: beam splitter; M1 and M2: high reflecting mirrors; CP: compensator plate; FL: focusing lens; QWP: quarter wave plate.

The frequency-doubled linear-polarized output of a regenerative Ti:sapphire amplifier with 1 kHz repetition rate and 100 fs pulse duration is used as the irradiation source. The wavelength of irradiation ($\lambda=400$ nm) is very close to the SP resonances of the NPs. The experimental setup that creates time-delayed pulse pairs is shown in Fig. 2. The input pulse is divided by a beam splitter into two pulses of equal energy, where one pulse is delayed with respect to the other by help of a motorized delay stage. As a result, pulse pairs are created with a variable Δt in between. The pairs of pulses are focused on the sample to a spot size of about $100 \mu\text{m}$, resulting in an energy density of $20 \text{ mJ}/\text{cm}^2$ per pulse. Moving the sample continuously on a motorized X-Y translation stage, a separate area is irradiated (written) for each desired delay between pulse pairs. The sample movement is arranged such that on average 300 pulse pairs hit one spot.

In standard configuration, the polarization of the pulse pair is linear with the polarization planes being parallel to each other. By inserting a quarter-wave plate in one arm of the setup, the pulse in this arm experiences a rotation of the plane of polarization by 90° . Thus, in this configuration, pulse pairs with linear but, with respect to each other, orthogonal polarization are produced.

After the pulse-pair irradiations, the samples were annealed for 1 h at 200°C in order to remove any possible laser-induced defects in the glass matrix.²² Then the polarization-dependent extinction bands from each irradiated area (representing one time delay Δt) are recorded by conventional transmission spectroscopy. These bands are then analyzed by the method of moments,²⁶ which is a statistical method allowing an objective comparison of the spectral parameters of extinction bands. The first moment defines the central position of a band; the second moment represents its bandwidth. “P-pol” (“S-pol”) abbreviate in the following polarization of light parallel (orthogonal) to the polarization of the second pulse of each pair interacting with the sample.

IV. RESULTS OF PULSE-PAIR IRRADIATION EXPERIMENTS

As mentioned before the original SP band of the spherical silver NPs is split into two polarization-dependent bands

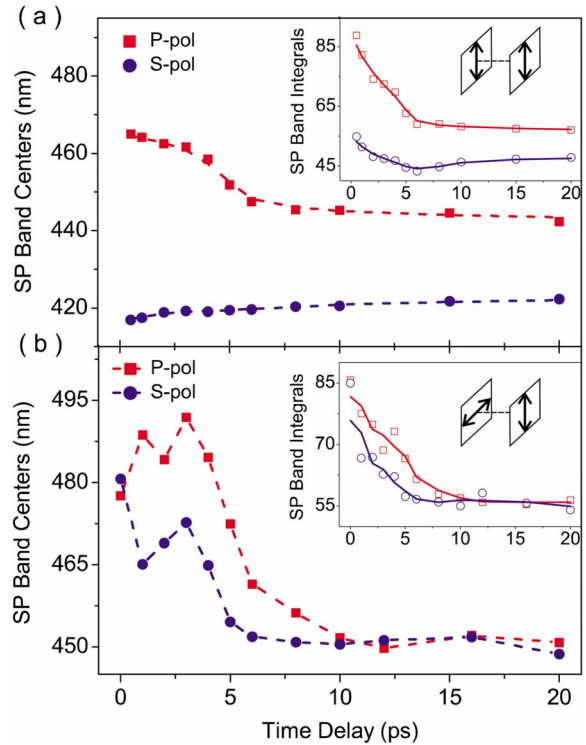


FIG. 3. (Color online) Time evolution of SP band centers for (a) parallel-polarized and (b) orthogonal-polarized pulse-pair irradiations. The insets of (a) and (b) are the corresponding time evolution of SP band integrals. All lines are given as a guide to the eye.

upon irradiation with a train of parallel-polarized pulses. The spectral gap between these polarized bands is related to the aspect ratio of the modified NP.^{3,27} Using the technique of pulse-pair irradiation, we found that the spectral gaps, and therefore also the NP shapes, depend strongly on the time delay between the two pulses of each pair.

The temporal evolution of the SP band centers for P-pol and S-pol are presented in Figs. 3(a) and 3(b) for the irradiation cases of parallel and orthogonal-polarized pulse pairs, respectively. Figure 3(a) shows that the maximum amount of dichroism (spectral band separation) is achieved for irradiation with pulse pairs following each other very quickly. For time delay larger than $\Delta t \approx 3$ ps, the P-band position shifts to smaller while the S-band position slightly toward longer wavelengths. At $\Delta t \approx 10$ ps, this decrease in the induced dichroism stops; for larger Δt the positions of the SP bands (spectral gap) remain almost unchanged. For the band integrals [inset of Fig. 3(a)], which are representing the total absorption of the NP system, the situation is different: directly after delay time $\Delta t=0$, both band integrals start to decrease until $\Delta t \approx 5$ ps. At larger temporal distance of the pulse pair, the P-pol band integral remains constant while the S-pol band integral is slightly recovering. Over all, the total absorption is significantly reduced when the delay between the two pulses is increased to 5 ps or more.

Figure 3(b) presents the results of a comparable series of experiments applying orthogonally polarized pulse pairs. The first important feature is observed at time delay zero, where the temporally overlapping pulses lead to a considerable red-shift of the SP band centers with respect to the original SP

band but without any directional preference. This behavior is the same as was obtained by irradiation of the NPs with circularly polarized pulses, which created a redshift of the SP band but no dichroism within experimental accuracy.⁶ However, already at a time delay of $\Delta t=1$ ps between the two pulses, dichroism with a considerable spectral gap of >20 nm occurs. Strikingly, the stronger redshifted SP band is found for polarization parallel to that of the second-hitting pulse. That means that also the nanoparticles' long axes are being defined by the pulse interacting with the sample later in time. This statement, however, is only true for a limited range of time delay: already for $\Delta t > 3$ ps the centers of both *s* and *p* bands start to experience smaller redshift upon irradiation, and a smaller spectral gap is produced. These trends continue until at $\Delta t=10$ ps the dichroism vanishes (spectral gap ≈ 0 nm); after this time delay the situation remains unchanged. The band integrals [inset of Fig. 3(b)] decrease similar to the case of Fig. 3(a), and also reach a stable situation at their minimum values around $\Delta t=10$ ps.

Comprising the above given results, we can give a first qualitative interpretation. Obviously the first pulse initiates ultrafast processes changing the state of the NP and its surrounding strongly during the first few picoseconds. With increasing time delay Δt , the second pulse causes a monotonous decrease in the band integrals, which is most plausibly explained by volume shrinking (partial dissolution) of NPs. This indicates, together with the behavior of the band centers in the case of orthogonal-polarized pulses, an isotropic process—tentatively ion emission—which prevents the second pulse from creating a directional memory for NP reshaping. The band centers show the largest spectral gaps for time delay $\Delta t \leq 3$ ps; in the case of orthogonal-polarized pairs the second pulse can redirect the directional memory within this interval of time. Most probably, these observations can be attributed to the directed electron emission. Therefore these processes will be in the focus of the following discussion.

V. DISCUSSION

To account for the temporal behavior seen in the experimental results, we now consider the relative probabilities of PETE and ITE of electrons for the cases of parallel and orthogonal-polarized pulse-pair irradiations. Starting point is again the two-temperature model, which is now applied to estimate the electronic temperatures for the case of pulse-pair irradiation of a NP. The inset of Fig. 4(a) shows the resulting time evolution of electronic and lattice temperature calculated for the case of irradiation with a pulse pair (energy matching the experimental values) at a time delay of 5 ps. As easily seen, the second pulse hitting the already hot NP increases the electronic temperature again; however, it is not as prominent as the first pulse effect because of the increased electron heat capacity. It is also observed that this further increase in T_e causes the lattice temperature to rise more steeply. To estimate the relative contributions of PETE and ITE processes, we applied the same procedure as described in Sec. II, i.e., calculated the percentage of electrons at >2.6 eV above the Fermi level as a function of time. Figure 4(a) shows as an example the result for a time delay Δt

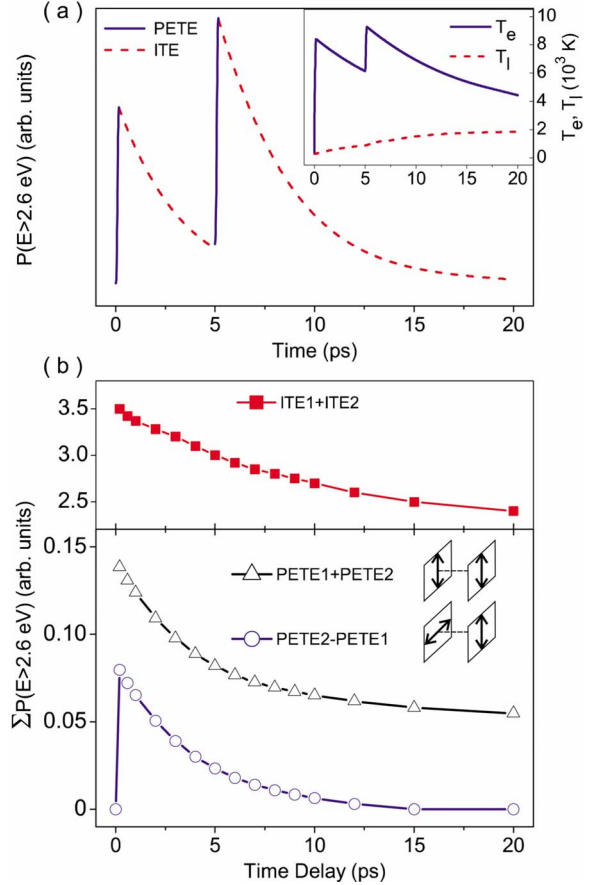


FIG. 4. (Color online) Inset of (a): time evolution of electronic and lattice temperatures for pulse-pair irradiation with $\Delta t=5$ ps. (a) The corresponding probabilities of electrons that possess energies above 2.6 eV. (b) Added probabilities of ITE and PETE for selected delay times.

$=5$ ps between the two pulses. Integrating over the time intervals where a laser field is present yields the total relative probability for the PETE processes during first and second pulses [regions indicated by blue solid lines in Fig. 4(a)]. Integration over the remaining time (no laser field) gives the total relative probability for ITE processes [regions indicated by red dashed lines in Fig. 4(a)]. Performing this procedure for the whole range of time delay between pulse pairs from perfect overlapping at $\Delta t=0$ ps to a maximum delay of 20 ps, the total relative probabilities of PETE and ITE processes are obtained as a function of the temporal sequence of the two pulses.

Now we have to compare these calculated numbers with the experimental results presented above. Experimentally, we have investigated the two cases of parallel and orthogonal polarizations of the pulse pairs, which imply a characteristic difference: the integrated probability of ITE processes does only depend on the current electronic temperature and thus the total amount of absorbed energy but is not at all sensitive to the laser-pulse polarization. In contrast, the PETE processes were assumed to be field-driven, i.e., to produce a directional distribution of electron emission which reflects the actual laser polarization. With respect to this definition, the amount of anisotropy initiated by the PETE processes in

case of parallel polarization of the pulse pair must be related to the sum of the PETE probabilities. For orthogonal polarization of a pulse pair, one expects a relation to the difference of PETE probabilities because directed emission of exactly the same amount of electrons in parallel and perpendicular directions cannot produce anisotropy of lowest (dipolar) order.

According to these considerations, Fig. 4(b) shows the integrated probability for ITE processes only once (upper panel) while in the lower panel both sum (open triangles) and difference (open circles) of the PETE probabilities, integrated separately over first (PETE1) and second pulse (PETE2), are plotted. It is most instructive to look at the difference first: while at $\Delta t=0$ the two contributions cancel each other as expected, already a few 100 fs time delay of the pulses leads to a clear prevalence of pulse-enhanced electron emission probability due to the second pulse. This can easily be explained by the fact that the second pulse can interact with an already very hot-electron system. With increasing Δt , the difference decreases down to zero at $\Delta t \approx 15$ ps. Over all, this behavior almost perfectly matches the experimentally observed dichroism as a function of Δt [Fig. 3(b)], as well as the finding that the second of two energetically equal pulses defines the direction of anisotropy. It is obvious to conclude that pulse-enhanced thermal emission of electrons into the matrix is the key process initiating the directional memory for the following shape transformation of the Ag nanoparticles.

This interpretation is confirmed considering the sum (PETE1+PETE2): first, the larger values of the total PETE probability corresponds nicely to the larger amount of anisotropy (spectral gap) observed for parallel-polarized pulse pairs. Second, the sum decreases by more than a factor of 2 when the pulse delay increases from very small Δt to $\Delta t \approx 10$ ps; the experimentally observed reduction in the spectral gap of the SP bands happens on the same time scale.

We can now consider which physical processes cause the reduction or even disappearance (for orthogonal-polarized pulse pairs) of the anisotropy within 10 ps. Clearly the purely thermal emission of electrons (ITE) is the first candidate: when isotropic injection of electrons into the glass has been going on long enough, all available trapping sites close to the NP will be occupied. Electrons emitted by a second pulse interacting after this time can, if at all, only be trapped at sites further away from the NP. For parallel-polarized pulse pairs, these sites are also already occupied by PETE during the first pulse so the electrons emitted by the second one will diffuse back to the NP, and as a result the anisotropy is not increased. In case of orthogonal-polarized pulse pairs, there are free sites in the emission direction, and the anisotropy can be cancelled. So, already this simplified scenario of saturation of the trapping sites can provide a reasonable explanation for the observed dependence of the dichroism on the pulse delay time Δt .

There are, however, further processes which might start within the first picoseconds after the laser-pulse interaction. In particular, any process of electron emission (no matter if directed or isotropic) ionizes the NP, rapidly creating repulsive Coulomb forces among the silver cations. Together with strongly increased temperature, this finally leads to emission

of ions (known as Coulomb explosion), reducing the total volume of a NP. For small Na clusters the typical time scale for Coulomb explosion is 0.5–1 ps.¹⁶ It is reasonable to assume a somewhat slower time scale for the emission of Ag ions from our comparably large NPs embedded in a rigid matrix. This is well compatible with the experimentally observed decrease in the SP band integrals as function of the pulse-pair delay Δt . So we can conclude that also ion emission at least starts within the first few picoseconds after interaction of the first pulse, and this will strongly change the state of both the NPs and of their surroundings. For instance, the dissipated kinetic energy of the Ag ions will lead to a fast temperature increase in the glass matrix close to the NP, which might remove the trapping sites for electrons. Also a loss of the silver crystal structure could result in a strongly modified reaction of the NP to the second laser pulse. All those secondary processes have the potential to prevent the preparation of an anisotropic distribution of trapped electrons, and offer plausible explanations that a second pulse coming in more than 10 ps after the first one cannot increase the produced persistent dichroism.

Summarizing this part, we want to point out that our investigation gave evidence that field-driven emission of hot electrons into the glass matrix is the dominating starting process for the fs laser-induced reshaping of Ag nanoparticles. As discussed in previous work, the whole process of shape transformation requires several further cascaded mechanisms on increasingly slower time scales: emitted ions can be reduced by previously emitted trapped electrons; owing to the directional distribution of these electrons, this reduction happens mainly close to the poles of the NP. Due to the increased temperature of the glass matrix in the vicinity of the particle, mediated first by emitted electrons and ions, and then by normal heat conduction, the reduced Ag atoms may either diffuse back to and reaggregate with the original NP or form small silver clusters in its surroundings. Irradiating several hundred pulses, this gradually leads to the NP shape changes and the usually observed halo of small silver clusters.¹¹

We are currently performing extended series of pulse-pair experiments for the time delay range from >20 ps to 1 ns, and various pulse energies. Preliminary results show that there are several further spectral changes on this longer time scales, which should provide additional insight in the physical mechanisms of NP shape transformation. The results of these investigations will be discussed in detail in a forthcoming publication.

VI. CONCLUSION

We have studied the initial stage of the NP shape modification dynamics by 100 fs pulse-pair irradiation experiments, restricted to a time delay range of $\Delta t \leq 20$ ps. Together with two-temperature model calculations, which have been extended to be valid also for very high temperatures, it was shown that directed electric field-driven emission of hot electrons, which are then trapped in the glass matrix, is the key process initiating the transformation of Ag nanoparticles to nonspherical shapes. This directional memory, which is pre-

pared only during the time of laser-pulse interaction, defines the anisotropy of the whole much longer-lasting process leading to ellipsoidal NPs and persistent dichroism, respectively. The anisotropic pulse-enhanced electron emission is counteracted by thermal isotropic electron emission and most probably Ag ion emission occurring on a timescale of a few picoseconds. This explains perfectly why the largest NP aspect ratios are being produced when the delay between pulse pairs is less than ≈ 3 ps. Thinking of the technological applications of laser-induced dichroism, it can be concluded that ultrashort pulses up to a duration of several picoseconds are well suited to prepare large spectral gaps between the polarized SP bands while the use of significantly longer pulses will favorably create the isotropic changes up to par-

ticle destruction. This conclusion is in full agreement with previous works.^{28,29}

Finally, the introduced technique proves to be a valuable tool to investigate the NP shape modification dynamics or, more generally, any ultrafast laser-induced processes which lead to irreversible optical changes. Time-delayed pulse-pair irradiation can provide additional information compared to usual pump-probe spectroscopy in these cases of the metal NPs.

ACKNOWLEDGMENTS

The authors thank Deutsche Forschungsgemeinschaft through SFB 418 for financial support and Codixx AG for the samples.

*heinrich.graener@physik.uni-halle.de

- ¹U. Kreibig and M. Vollmer, *Optical Properties of Metal Clusters* (Springer, Berlin, 1995).
- ²S. Link and M. A. El-Sayed, *J. Phys. Chem. B* **103**, 8410 (1999).
- ³K. L. Kelly, E. Coronado, L. L. Zhao, and G. C. Schatz, *J. Phys. Chem. B* **107**, 668 (2003).
- ⁴V. M. Shalaev and S. Kawata, *Nanophotonics with Surface Plasmons* (Elsevier, Amsterdam, 2007).
- ⁵M. Kaempfe, T. Rainer, K. J. Berg, G. Seifert, and H. Graener, *Appl. Phys. Lett.* **74**, 1200 (1999); **77**, E459 (2000).
- ⁶M. Kaempfe, G. Seifert, K. J. Berg, H. Hofmeister, and H. Graener, *Eur. Phys. J. D* **16**, 237 (2001).
- ⁷A. Arbouet, C. Voisin, D. Christofilos, P. Langot, N. Del Fatti, F. Vallee, J. Lerme, G. Celep, E. Cottancin, M. Gaudry, M. Pellarin, M. Broyer, M. Maillard, M. P. Pileni, and M. Treguer, *Phys. Rev. Lett.* **90**, 177401 (2003).
- ⁸C. Voisin, D. Christofilos, P. A. Loukakos, N. Del Fatti, F. Vallee, J. Lerme, M. Gaudry, E. Cottancin, M. Pellarin, and M. Broyer, *Phys. Rev. B* **69**, 195416 (2004).
- ⁹M. Perner, S. Gresillon, J. Marz, G. von Plessen, J. Feldmann, J. Porstendorfer, K. J. Berg, and G. Berg, *Phys. Rev. Lett.* **85**, 792 (2000).
- ¹⁰A. Stalmashonak, G. Seifert, and H. Graener, *Opt. Lett.* **32**, 3215 (2007).
- ¹¹A. Stalmashonak, A. Podlipensky, G. Seifert, and H. Graener, *Appl. Phys. B: Lasers Opt.* **94**, 459 (2009).
- ¹²P. V. Kamat, M. Flumiani, and G. V. Hartland, *J. Phys. Chem. B* **102**, 3123 (1998).
- ¹³T. Doppner, T. Fennel, T. Diederich, J. Tiggesbaumker, and K. H. Meiwes-Broer, *Phys. Rev. Lett.* **94**, 013401 (2005).
- ¹⁴G. Seifert, M. Kaempfe, K. J. Berg, and H. Graener, *Appl. Phys. B: Lasers Opt.* **71**, 795 (2000).
- ¹⁵E. Hao, G. C. Schatz, and J. T. Hupp, *J. Fluoresc.* **14**, 331 (2004).
- ¹⁶F. Calvayrac, P. G. Reinhard, E. Suraud, and C. A. Ullrich, *Phys. Rep.* **337**, 493 (2000).
- ¹⁷J. Y. Bigot, V. Halte, J. C. Merle, and A. Daunois, *Chem. Phys.* **251**, 181 (2000).
- ¹⁸S. I. Anisimov, B. L. Kapeliovitch, and T. L. Perelman, *Sov. Phys. JETP* **39**, 375 (1974).
- ¹⁹O. L. Muskens, N. Del Fatti, and F. Vallee, *Nano Lett.* **6**, 552 (2006).
- ²⁰Z. Lin, L. V. Zhigilei, and V. Celli, *Phys. Rev. B* **77**, 075133 (2008).
- ²¹R. Hultgren, P. D. Desai, D. T. Hawkins, M. Gleiser, K. K. Kelley, and D. D. Wagman, *Selected Values of the Thermodynamic Properties of the Elements* (American Society for Metals, Ohio, 1973).
- ²²A. V. Podlipensky, V. Grebenev, G. Seifert, and H. Graener, *J. Lumin.* **109**, 135 (2004).
- ²³G. Mie, *Ann. Phys.* **330**, 377 (1908).
- ²⁴C. Bohren and D. Huffmann, *Absorption and Scattering of Light by Small Particles* (Wiley, New York, 1983).
- ²⁵B. N. J. Persson, *Surf. Sci.* **281**, 153 (1993).
- ²⁶G. G. Dyadyusha and A. A. Ishchenko, *J. Appl. Spectrosc.* **30**, 746 (1979).
- ²⁷J. Porstendorfer, K. J. Berg, and G. Berg, *J. Quant. Spectrosc. Radiat. Transf.* **63**, 479 (1999).
- ²⁸G. Seifert, M. Kaempfe, K. J. Berg, and H. Graener, *Appl. Phys. B: Lasers Opt.* **73**, 355 (2001).
- ²⁹F. Gonella, G. Mattei, P. Mazzoldi, E. Cattaruzza, G. W. Arnold, G. Battaglin, P. Calvelli, R. Polloni, R. Bertinello, and R. F. Haglund, Jr., *Appl. Phys. Lett.* **69**, 3101 (1996).